

High-accuracy differential thermal analysis: A tool for calorimetric investigations on small high-temperature-superconductor specimens

A. Schilling and O. Jeandupeux

Laboratorium für Festkörperphysik, Eidgenössische Technische Hochschule Hönggerberg, 8093 Zürich, Switzerland

(Received 4 May 1995)

We describe a technique for measuring small heat capacities below room temperature, which represents a simple but significant improvement of the conventional differential thermal-analysis (DTA) method by means of high-precision electronic components. It is thereby possible to measure the heat capacity $C(T)$ of milligram samples with a relative accuracy $\delta C/C < 0.02\%$. This simple and fast DTA method is suitable not only to detect the specific-heat discontinuity at T_c of high-temperature superconductors, but also to study the thermodynamics at the irreversibility boundary $H_{\text{irr}}(T)$ in the magnetic phase diagram of cuprate superconductors. From respective measurements on a $\text{YBa}_2\text{Cu}_3\text{O}_7$ single crystal, we deduce an upper limit for a latent heat L associated with a hypothetical first-order transition at $H_{\text{irr}}(T)$, namely $L < 0.05k_B T$ per vortex per layer for an external field $\mu_0 H = 7$ T parallel to the c axis of the investigated specimen.

I. INTRODUCTION

The electronic specific heat of cuprate superconductors is the subject of many recent experimental studies.¹⁻⁹ The interpretation of corresponding heat-capacity $C(T)$ data taken in the superconducting state is still controversial, however.^{5,7,10} In order to come to a conclusive interpretation of experimental data, a lot of efforts have been made to improve the precision of such measurements.

It is a fact that the classical heat-pulse method for measuring heat capacities is not adequate to resolve discontinuities in the specific heat at the critical temperature T_c of copper oxide superconductors, which are typically of the order of 3% of the total signal or less due to the dominant phonon background at these temperatures.

Sufficiently accurate results for relative changes in the heat capacity have been obtained in ac calorimetry experiments,^{1,2,7} in which signal averaging over time allows a very precise evaluation of variations in $C(T)$, especially for small samples (i.e., sample masses less than 1 mg).¹¹ Unfortunately, such techniques are rather time consuming, and absolute $C(T)$ values cannot be reliably obtained.

One of the best methods operating at temperatures of the order of T_c (i.e., around $T=100$ K) is the continuous-heating technique,¹² in which the temperature evolution of the sample due to a continuous heat supply is used to calculate $C(T)$. Such experiments yield specific-heat data of high absolute and relative accuracy ($\approx 1\%$ and $< 0.02\%$, respectively³), with an impressive data-point density on the temperature scale. Although the investigated specimens need not be extremely large, sample masses larger than 100 mg are usually required. Moreover, a certain technical effort has to be made to maintain perfectly adiabatic conditions.

Special electrical-regulation circuitry is also needed in one version of a differential calorimeter, in which the heating power is adjusted such as to maintain zero tem-

perature difference between the sample and a reference sample with known heat capacity.⁹ This technique has been reported to yield very accurate results, but sample masses of the order of grams are required.

At temperatures well below T_c , where large internal equilibrium times make the use of ac or continuous-heating techniques impracticable, the relaxation technique has been proven to be one of the most reliable methods for determining heat capacities. In such experiments, the temperature relaxation of a sample due to a calibrated heat link to a thermal bath is monitored as a function of time.¹³ The relatively large time constants involved make these experiments time consuming, and the absolute accuracy of respective heat-capacity data is somewhat limited for sample masses smaller than ≈ 10 mg, however.

A more qualitative tool for investigating the thermodynamics of chemical reactions and phase transitions is the differential thermal-analysis (DTA) technique, which is widely used in chemical and material sciences. In a typical experiment, the specimen and a reference material of similar heat capacity are heated simultaneously. If the two samples are sufficiently thermally insulated from each other, changes in the temperature difference between the sample and the reference material reflect heat-capacity variations or indicate the occurrence of chemical reactions. Typical heating rates are of the order of several degrees per minute. Under such conditions, however, the samples are not always in thermal equilibrium. The resulting problems with the geometry of the samples and the sample holders make a calculation of absolute heat-capacity data rather complicated, and it is therefore rarely done in practice.¹⁴

In this paper, we describe how to use the standard experimental configuration of the DTA technique to obtain very accurate heat-capacity data below room temperature. The use of high-precision electronic components makes it possible to achieve a relative accuracy

$\delta C/C < 0.02\%$ in the heat capacity C on samples of milligram size, independent of the strength of an externally applied magnetic field. This accuracy is at least of the same order of magnitude as that reached with the frequently used continuous-heating technique, where significantly larger sample masses are usually required. Moreover, the method is time saving and very simple to apply since neither circumstantial calibration work nor a very precise temperature regulation is necessary in principle. Heat-capacity measurements can be done upon heating or cooling the samples. This allows us, for example, to take data while cooling a specimen in an external magnetic field.

In the first part of the paper, we will discuss how heat-capacity $C(T)$ data can be obtained from such DTA experiments (Sec. II), and how a first-order phase transition can be identified in general (Sec. III). In the second part we will present the respective results from measurements of the heat capacity on monocrystalline $\text{YBa}_2\text{Cu}_3\text{O}_7$ around the transition to superconductivity in order to demonstrate the efficiency of the technique presented here (Sec. IV). In Sec. V we will finally give an upper limit for the latent heat L associated with a hypothetical first-order transition at the irreversibility boundary $H_{\text{irr}}(T)$ for external fields H parallel to the c axis of the investigated crystal.

II. THE PRINCIPLE OF THE MEASUREMENT

A schematic view of the standard DTA configuration used for the present work is shown in Fig. 1. The sample (with heat capacity C_s at a temperature T_s) and a reference sample (at a temperature T_r with known heat capacity C_r) are thermally connected to a heat reservoir (temperature T_b) via the heat links k_s and k_r , respectively. The experimental realization of these heat links is not relevant for the following calculation (see below). For completion we may also include a thermal connection k_{rs} between the sample and the reference object although it is possible to thermally isolate the two specimens from each other in a real experiment, i.e., $k_{rs} \ll k_s$ and k_r . Results of a calculation taking the effect of a nonzero k_{rs} into account are discussed in an Appendix to this paper.

If the temperature of the thermal bath T_b varies with time, we may describe the system according to the equations

$$C_s \dot{T}_s = k_s (T_b - T_s), \quad (1a)$$

$$C_r \dot{T}_r = k_r (T_b - T_r). \quad (1b)$$

A. Steady-state approximation

It is instructive to first consider steady-state solutions of Eqs. (1) when C_s and C_r are assumed to be temperature independent, and $T_b(t)$ is a linear function of time. In order to avoid the above-mentioned thermal-equilibrium problems in the present version of DTA experiments, we choose the characteristic time constants of the system, $\tau_j = C_j/k_j$ (with $j=s$ or r) to be larger than the internal equilibrium times of the samples, τ_{int} , which are typically

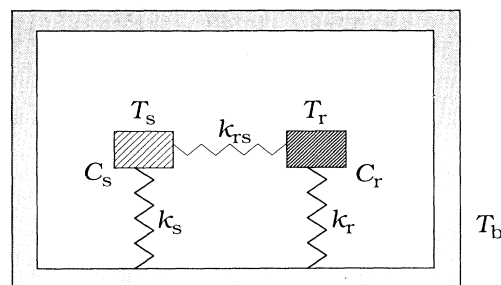


FIG. 1. Schematic view of the standard DTA configuration used for the present work. The sample (heat capacity C_s , temperature T_s) and a reference sample (heat capacity C_r , temperature T_r) are thermally connected to a heat reservoir (temperature T_b) via the heat links k_s and k_r . The effect of an additional unwanted link k_{rs} is discussed in an Appendix to this paper.

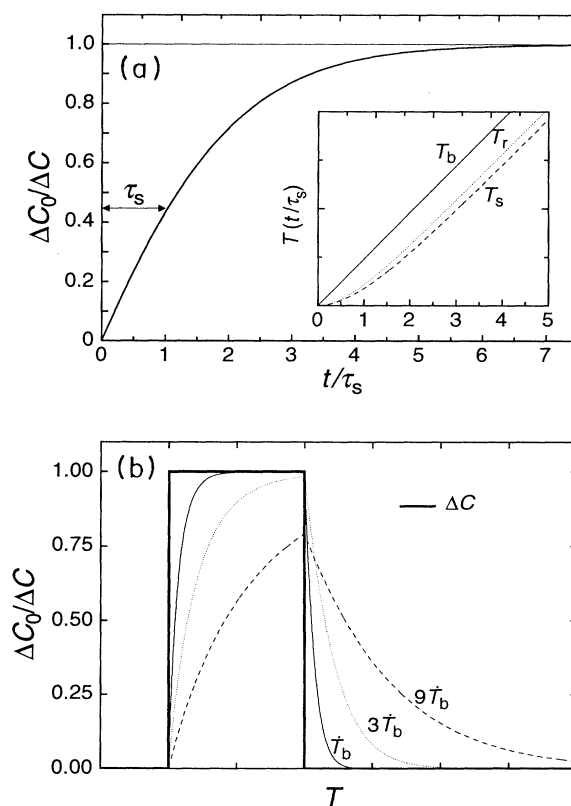


FIG. 2. (a) Evolution of the quantity ΔC_0 calculated according to Eq. (2) (in units of the effective heat-capacity difference ΔC , here assumed to be constant), as a function of time t (in units of the time constant $\tau_s = C_s/k_s$). ΔC_0 asymptotically approaches ΔC for $t \gg \tau_s$. The inset shows the respective time dependence of the temperatures T_s and T_r . T_b has been chosen to vary linearly with time. (b) Influence of the heating rate \dot{T}_b on the quantity ΔC_0 when crossing a sharp feature in the heat-capacity difference ΔC (thick solid line), qualitatively plotted on an arbitrary temperature scale.

less than $\tau_{\text{int}}=1$ s at $T=100$ K (see below). We obtain in a straightforward way $\dot{T}_s=\dot{T}_r=\dot{T}_b$, and $T_b-T_j=C_j\dot{T}_b/k_j$. Assuming identical heat links, i.e., $k_s=k_r$, we find that the quantity

$$\Delta C_0=C_r \left[\frac{T_s-T_r}{T_r-T_b} \right] \quad (2)$$

approaches asymptotically the heat-capacity difference $\Delta C=C_s-C_r$ at times $t \gg \tau_j$ after switching on the linear temperature ramp $T_b(t)$ [see Fig. 2(a)]. In a more realistic scenario, the heat capacities C_s and C_r are temperature dependent, and $T_b(t)$ can deviate from linearity. It may then be argued that ΔC_0 still approaches ΔC for $t \gg \tau_j$ as long as heat-capacity changes and variations of \dot{T}_b in time are sufficiently slow, i.e., occur on a time scale much larger than τ_j .

It is very easy to measure the temperatures T_s , T_r , and T_b in an experiment. If $k_s=k_r$, ΔC_0 calculated according to Eq. (2) (hereafter often denoted as "raw data") represents an excellent approximation for the heat-capacity difference ΔC , and can be determined without knowledge of the absolute values of k_s and k_r .

A sharp feature in the quantity C_s and thus in ΔC will be smeared out due to the finite thermal relaxation of the system, however. This occurs on the time scale $\tau_s=C_s/k_s$. Within this time the sample will be heated by $\delta T=\tau_s\dot{T}_s \approx \tau_s\dot{T}_b=T_b-T_s$, which is therefore a measure for the resulting broadening effect on $\Delta C_0(T)$ on the temperature axis [see Fig. 2(b)]. According to Eq. (2), heat-capacity differences ΔC with respect to a known reference capacity C_r can be determined within this instrumental uncertainty simply by simultaneously monitoring the temperature differences T_s-T_r and T_r-T_b , *without calculating any derivative in time or in temperature*. The above-mentioned limit $|T_b-T_s|$ in the instrumental temperature resolution for $\Delta C_0(T)$ can be reduced by slowing down the variation $T_b(t)$ of the heat reservoir since $T_b-T_s=C_s\dot{T}_b/k_s$ [see Fig. 2(b)].

B. Exact results

Without a knowledge of the general exact solutions for $T_s(t)$ and $T_r(t)$ we can nevertheless find an *exact* relation for the heat-capacity difference

$$\Delta C=C_s-C_r=\frac{k_s}{k_r} \frac{\dot{T}_r}{\dot{T}_s} C_r \left[\frac{T_s-T_r}{T_r-T_b} + 1 \right] - C_r, \quad (3)$$

and hence

$$C_s=\Delta C+C_r=\frac{k_s}{k_r} \frac{\dot{T}_r}{\dot{T}_s} (\Delta C_0+C_r). \quad (4)$$

The ratio \dot{T}_r/\dot{T}_s is exactly one for a steady-state solution of Eqs. (1) (see above). It may deviate from unity when sudden heat-capacity changes occur, or more generally under non-steady-state conditions, e.g., after starting the temperature ramp $T_b(t)$. The above-mentioned broadening in temperature of $\Delta C_0(T)$ raw data by $|T_b-T_s|$ is a direct consequence of fixing $\dot{T}_r/\dot{T}_s=1$ in Eq. (2). It can

thus be eliminated in principle by calculating the time derivatives \dot{T}_s and \dot{T}_r from experimental $T_s(t)$ and $T_r(t)$ data, respectively, and inserting these quantities in Eq. (4).

Note that in the above calculation it was *not* required that the heat capacities C_s and C_r are similar. In this sense Eq. (4) represents an exact relation obeyed by any solutions $T_s(t)$ and $T_r(t)$ of Eqs. (1) for arbitrary $C_s(T)$, $C_r(T)$, and $T_b(t)$, even far from steady-state conditions.

C. Absolute accuracy of heat-capacity $C_s(T)$ data

A discussion about the absolute accuracy of heat-capacity C_s values has to include the case $k_s \neq k_r$. From Eq. (4) it is clear that an uncertainty in the ratio k_s/k_r leads to an error in the absolute value of the total heat capacity C_s as well as in ΔC . In practice it is somewhat difficult to fabricate two exactly identical heat links to the heat reservoir, especially when experiments are done at high temperatures where an additional heat transfer due to thermal radiation has to be taken into account. In an experiment such links may consist, for example, of thin metallic wires with cross section S_w , length l_w , and thermal conductivity λ_w , so $k_{\text{wire}}=\lambda_w S_w/l_w$. If the thermally conducting wires are made of the same material, the ratio k_s/k_r should not depend on temperature as long as thermal radiation is negligible. At high temperatures T_b , however, this radiation may dominate the thermal conduction of the wires, i.e., $k_{\text{rad}} \approx 4A\sigma ST_b^3 \gg k_{\text{wire}}$, where A is the emissivity factor of the specimen surface S , and $\sigma=5.67 \times 10^{-8} \text{ W m}^{-2} \text{ K}^{-4}$. The ratio k_s/k_r should then again be approximately temperature independent. In between these two extreme cases, k_s/k_r may vary smoothly as a function of temperature between the two limiting values. To minimize the uncertainty about this factor, it is necessary to make the thermal connections as identical as possible. It is also preferable to choose a reference specimen with a surface similar to that of the sample under investigation. Without these experimental precautions regarding the heat-link ratio k_s/k_r , very accurate absolute values for C_s cannot be obtained. Luckily it is not necessary to have a knowledge about the individual values of k_s and k_r .

A very reasonable approach for handling the problem of an unknown heat-link ratio k_s/k_r is to calculate the quantity ΔC_0+C_r using Eq. (2) and compare the result with reliable reference data C_s for the sample material at selected temperatures, if such data are available. According to Eq. (4) the two sets of data essentially differ by the factor k_s/k_r . The raw data ΔC_0+C_r may now be multiplied, if necessary, by a smooth function fitting the temperature-dependent k_s/k_r values thus obtained. Such a procedure recalls data-correction techniques used to treat corresponding raw data from ac calorimetry experiments. The correction is not drastic in the present DTA technique, however, if the heat links are reasonably well constructed. For the experimental data to be presented below, corrections of that kind have been estimated to be smaller than 5% of the total heat capacity.

D. Relative scatter of heat-capacity $C_s(T)$ data and the instrumental broadening on the temperature scale

The relative scatter in ΔC_0 raw data is essentially determined by the experimental resolution in $T_s - T_r$ and $T_r - T_b$, respectively [see Eq. (2)]. If the reference material does not show any discontinuity in its heat capacity C_r (here assumed to be an exactly known quantity), experimentally measured $T_r(t) - T_b(t)$ values can be safely substituted by a smoothly fitted function since $T_r - T_b$ is essentially proportional to C_r . It is therefore obvious that in practice a scatter in the raw data ΔC_0 is related only to a corresponding uncertainty in $T_s - T_r$. If we are able to measure this difference with a certain temperature resolution θ , the relative scatter in $\delta\Delta C_0/C_r$ will be of the order of $\theta/(T_r - T_b)$. Slowing down the temperature variation $T_b(t)$ with the aim of reducing the above-discussed instrumental broadening $\delta T = |T_b - T_s| \approx |T_r - T_b|$ in temperature leads therefore to an inevitable increase in the scatter $\delta\Delta C_0/C_r$. The product of these two uncertainties, $\delta T \delta\Delta C_0/C_r \approx \theta$, is an instrumental constant fixed by the resolution θ for measuring $T_s - T_r$. Selecting $C_s \approx C_r$ will minimize the quantity $T_s - T_r$, which can then be measured using the highest accuracy range available on a suitable electronic device. It is only for this purpose that it is preferable to choose the reference heat capacity C_r as close as possible to the unknown heat capacity C_s .

Similar arguments can be used to show that the above discussed correction of measured ΔC_0 raw data by the factor \dot{T}_r/\dot{T}_s [see Eq. (4)] does not really lead to an improved overall accuracy of the measurement, $\delta T \delta\Delta C/C_r$, if the time derivatives are naively calculated according to the approximation $\dot{T}(t) \approx [T(t + \Delta t) - T(t)]/\Delta t$. The relative error introduced by such a calculation of \dot{T}_s and \dot{T}_r is of the order of $\delta\Delta C/C_r = \theta/\dot{T}_b \Delta t$, while the uncertainty in T remains $\delta T = \dot{T}_b \Delta t$, and hence $\delta T \delta\Delta C/C_r \approx \theta$. Nevertheless, a very significant improvement can be achieved by least-squares fitting of suitable smooth functions, e.g., polynomials, to the measured $T_s(t)$ and $T_r(t)$ data, respectively, and calculating the respective derivatives directly from these functions. With such a procedure, the smearing on the temperature axis in the raw data $\Delta C_0(T)$ can be essentially removed without enhancing the scatter $\delta\Delta C$ in the ΔC data corrected according to Eq. (4) (see below). In practice, it is the internal thermal relaxation time τ_{int} due to the finite thermal constants of the sample which defines a lower limit for the instrumental resolution in temperature, i.e., $\delta T > \tau_{\text{int}} \dot{T}_b$.

III. DETECTION OF A FIRST-ORDER PHASE TRANSITION

Let us now assume that the sample under investigation undergoes a first-order phase transition associated with a latent heat L at the transition temperature T^* . For simplicity we assume here $k_s = k_r$ and $C_s = C_r$. Although a certain heating power P is continuously supplied through the heat links, the sample temperature T_s remains con-

stant at T^* during a time Δt until $P\Delta t = L$. The reference material is heated at the same time by the temperature $\Delta T = P\Delta t/C_r$, or

$$\Delta T = \frac{L}{C_s}. \quad (5)$$

Consequently the temperature difference $|T_s - T_r|$ increases at $T_s = T^*$ by ΔT within the time Δt , and then decays as a function of time with the time constant τ_s or within $\approx |T_b - T_s|$ on the temperature axis, respectively. Most remarkably, the increase ΔT in $|T_s - T_r|$ given in Eq. (5) does not depend on the size of the investigated specimen since both L and C_s are proportional to the sample volume. In practice, however, the heat capacity C_s includes unwanted heat capacities due to mechanical suspension, heat links, and thermometers, with the effect of reducing ΔT to a certain extent. A shift in $T_s - T_r$ by ΔT may also be more easily located in experimental data when the time constant τ_s related to C_s is not too small. Nevertheless, a latent heat L should be well detectable also on very small specimens as long as the temperature resolution θ for measuring $T_s - T_r$ is sufficient, i.e., if $L/C_s > \theta$. Note that a knowledge of the heating power P is not necessary for an evaluation of $L = \Delta TC_s$ from corresponding $T_s - T_r$ data.

In thermodynamic equilibrium the heat capacity C_s is a well-defined quantity as a function of temperature T as long as no jump in entropy $\Delta S = L/T^*$ occurs. If the heating rate \dot{T}_b is small enough to allow the sample to come to an equilibrium, a feature in measured $\Delta C_0(T)$ raw data due to a higher-order phase transition should be independent of \dot{T}_b . A first-order phase transition at T^* characterized by a δ function $\hat{C}(T) = L\delta(T - T^*)$, however, will show up in experimental $\Delta C_0(T)$ data as a feature of variable amplitude $\Delta\hat{C}_0$, broadened around $T_s = T^*$ by the \dot{T}_b -dependent instrumental uncertainty $T_b - T_s$. According to the above discussion, it is the temperature difference $\Delta T = L/C_s$ in $|T_s - T_r|$, rather than the corresponding discontinuity $\Delta\hat{C}_0 \approx L/|T_b - T_s|$ at T^* , which is independent of the heating rate \dot{T}_b . Performing measurements according to the DTA technique described here using different temperature variations \dot{T}_b thus allows one to clearly identify a first-order phase transition associated with an entropy jump ΔS .

IV. SPECIFIC HEAT OF MONOCRYSTALLINE $\text{YBa}_2\text{Cu}_3\text{O}_7$ NEAR T_c

The experiments were done on an $\text{YBa}_2\text{Cu}_3\text{O}_7$ single crystal which was selected by virtue of its sharp transition to superconductivity [$\Delta T < 0.2$ K at $T_c \approx 91.4$ K (Ref. 15)]. Results from detailed measurements of its magnetic and transport properties have been previously published.^{15,16} The sample (with mass $m_s = 16.8$ mg) and a copper reference (99.999% purity, $m_r = 15.6$ mg) were attached to nylon filaments using a small amount (< 0.05 mg) of GE 7031 varnish. The temperature differences $T_s - T_r$, $T_r - T_b$, and $T_s - T_b$ were measured using similarly attached copper-Constantan thermocouples in a

differential configuration. The respective copper wires (50 μm diameter, ≈ 8 cm in length) were designed to act as heat links to the heat reservoir, while a thinner Constantan wire minimizing a possible related heat transfer (30 μm diameter, ≈ 10 cm in length) was used to connect the sample and the reference specimen (see the Appendix). The temperature T_b of the thermal bath, a massive copper can with a Constantan heater, was measured with a platinum thermometer which had been calibrated between 30 and 300 K, and in magnetic fields up to 7 T. The temperature T_b can be regulated to a target temperature within a relative accuracy of ± 1 mK, while the absolute accuracy on the temperature scale is ≈ 200 mK. In typical experiments, the variation $T_b(t)$ was chosen to be linear in time, with heating rates ranging from 1.5 to 6 mK/s. The time constants τ_s and τ_r were typically of the order of 120 s at $T=90$ K.

The voltage difference ΔV_{rs} related to $T_s - T_r$ was monitored with a Keithley 2001 voltmeter plus 1801 picovolt option. Using the voltmeter settings selected for the experiments described here, the scatter in the voltage ΔV_{rs} is typically of the order of 2 nV (peak to peak), with a voltmeter response time of approximately 0.5 s. This time constant is much smaller than τ_s and τ_r , and can therefore be safely neglected in the data analysis. The voltages ΔV_{rb} and ΔV_{sb} related to $T_r - T_b$ and $T_s - T_b$, respectively, were detected with an additional Keithley 2001 voltmeter in its highest sensitivity range with a 0.1 μV resolution. After applying offset corrections to be described below, all these voltages were transformed to temperature differences using a calibrated standard table, before inserting these quantities in the equations to evaluate $C_s(T)$. It should be noted, however, that no exact calibration of the thermocouples is necessary for a calculation of ΔC_0 because an error in the temperature- and field-dependent proportionality factor connecting the temperature differences and the corresponding voltage differences cancels out in Eq. (2).

The voltages ΔV_{rs} , ΔV_{rb} , and ΔV_{sb} had to be corrected by previously measured offset voltages due to parasitic thermal emf's of various origins. The shift in the larger voltages ΔV_{rb} and ΔV_{sb} ($\approx 20\mu\text{V}$) turned out to be a constant of the order of 4 μV , while the correction in the much smaller voltage ΔV_{rs} (≈ 1000 nV) was slightly temperature dependent. This correction was accurately measured by ramping the temperature $T_b(t)$ up and down with the same heating and cooling rate $|\dot{T}_b|$, respectively, and calculating the mean value of the thus obtained $\Delta V_{rs}(T)$ data [see Fig. 3(a)]. This is possible because the corrected voltage $\Delta V_{rs}(T)$ related to $T_s - T_r$ simply changes sign upon cooling, compared to similar data collected when heating the samples.

To obtain an estimate for the correction factor k_s/k_r discussed above, we first computed the quantity $\Delta C_0 + C_r$ according to Eq. (2). We used here the data from Ref. 17 for calculating the heat capacity $C_r(T)$ of the copper reference. We then compared the result with corresponding data that we measured separately on a larger $\text{YBa}_2\text{Cu}_3\text{O}_7$ specimen using the continuous-heating technique, which is known to yield very accurate absolute

heat-capacity data. The result of this comparison is shown in Fig. 3(b) (inset). The maximum deviation in absolute heat-capacity data between 45 and 130 K is only 5% [see Fig. 3(b)]. We therefore decided not to correct our data using these empirically estimated k_s/k_r values. We also did not attempt to make corrections accounting for the small heat capacities due to varnish, nylon, and thermocouple wires. In a symmetric configuration, these unwanted contributions cancel out in a first approximation.

The influence of a variation of the heating rate \dot{T}_b on the specific-heat $(\Delta C_0 + C_r)/T$ raw data is demonstrated in Fig. 4. It is obvious that a large heating rate leads to little scattered specific-heat data, while the relative scattering increases with decreasing \dot{T}_b . Inspecting the shape of the specific-heat discontinuity at T_c we also notice that the anomaly becomes sharper on the tempera-

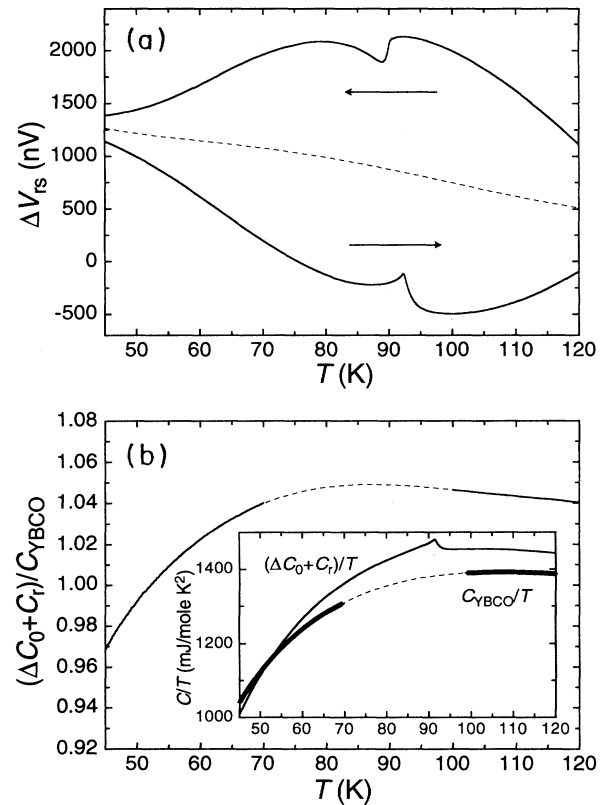


FIG. 3. (a) Measured voltage ΔV_{rs} as a function of temperature T for $\dot{T}_b = +6$ mK/s (lower branch) and -6 mK/s (upper branch), respectively. The dashed line represents the offset voltage in ΔV_{rs} that we extracted from these data (see text). (b) Ratio between the heat capacity $\Delta C_0 + C_r$, measured on a single crystal of $\text{YBa}_2\text{Cu}_3\text{O}_7$ according to the DTA technique discussed here [see Eq. (2)], and corresponding data that we obtained on another larger $\text{YBa}_2\text{Cu}_3\text{O}_7$ sample using the standard continuous-heating method. The latter $C_{\text{YBCO}}(T)$ data have been replaced by a third-order polynomial interpolation in a temperature window around T_c (dashed line) to obtain a smooth $(\Delta C_0 + C_r)/C_{\text{YBCO}}$ vs T curve. This ratio should correspond to the temperature-dependent heat-link ratio k_r/k_s (see text). The original data, plotted as C/T vs T , are shown in an inset.

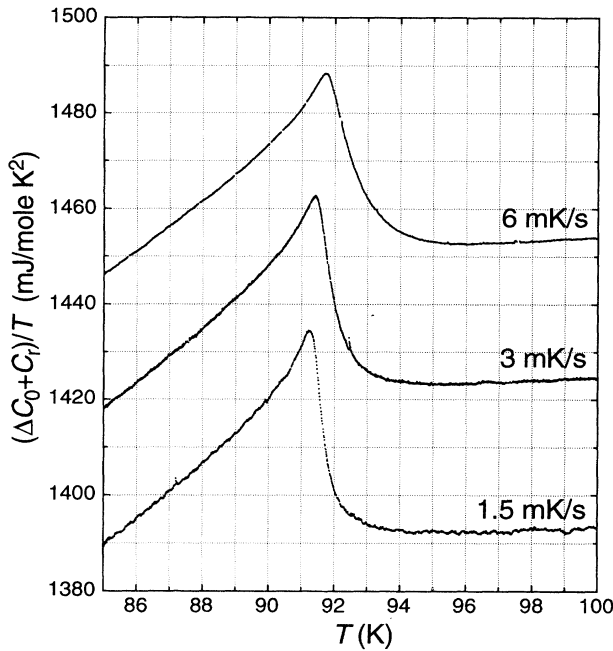


FIG. 4. Specific-heat $(\Delta C_0 + C_r)/T$ raw data around the transition to superconductivity T_c of $\text{YBa}_2\text{Cu}_3\text{O}_7$, calculated according to Eq. (2) from data that we obtained by using different heating rates \dot{T}_b . For clarity the curves for $\dot{T}_b = 3$ and 1.5 mK/s have been vertically shifted by -30 and -60 mJ/mole K^2 , respectively.

ture axis when using a small heating rate, in full accordance with the above discussion. The product of the respective instrumental uncertainties is $\delta T \delta \Delta C_0 / C_r \approx 0.2$ mK. Note that this value could be reduced in principle by applying suitable data-averaging techniques, which, however, has not been done for any of the data presented here.

In Fig. 5 we show a collection of specific-heat $(\Delta C_0 + C_r)/T$ raw data from another experiment, for various external magnetic fields H . These data were obtained while heating the heat reservoir with $\dot{T}_b = +6$ mK/s. It is obvious that the application of a magnetic field does not enhance the scatter in the heat-capacity data.

The result of a correction taking the ratio \dot{T}_r / \dot{T}_s from Eq. (4) into account is plotted in Fig. 6, where we have identified $C \equiv C_s$. These C/T data are, according to the above arguments, virtually free from broadening effects in temperature. This is nicely reflected in our data by the exceptional sharpness of the zero-field discontinuity at T_c . It is worth mentioning that due to the small internal equilibrium time of the sample investigated here, $\tau_{\text{int}} \approx 10^{-2}$ s, possible thermal gradients inside the sample are of the order of only $\tau_{\text{int}} \dot{T}_b \approx 0.1$ mK in all the experiments described here. The relative accuracy achieved in our measurements, $\delta C / C \approx 0.02\%$, is comparable to what is reached with the frequently used continuous-heating method.^{5,12} We want to point out, however, that the sample masses needed for our DTA experiments are an order of magnitude lower than what is routinely used

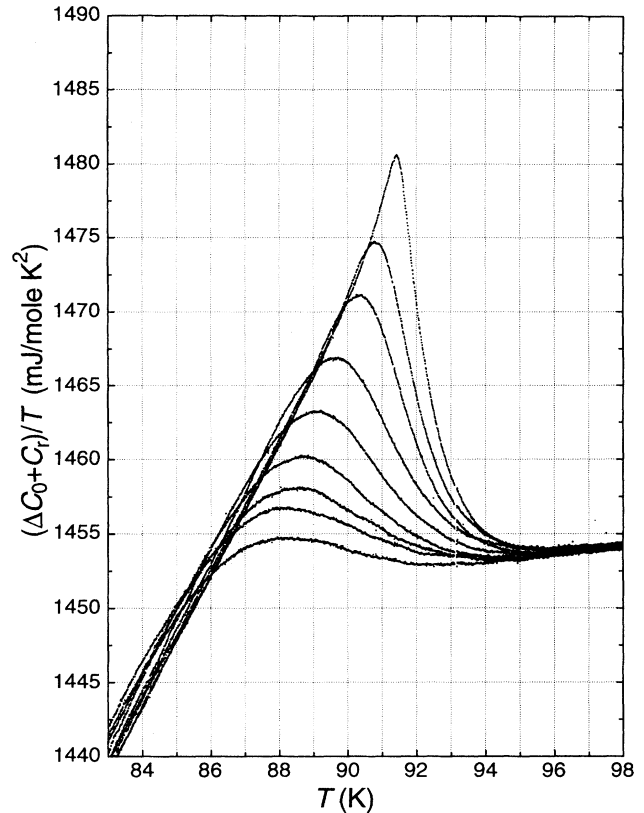


FIG. 5. Specific-heat $(\Delta C_0 + C_r)/T$ raw data near T_c of an $\text{YBa}_2\text{Cu}_3\text{O}_7$ single crystal, calculated according to Eq. (2). The different curves (from top to bottom) correspond to external magnetic fields $\mu_0 H = 0, 0.5, 1, 2, 3, 4, 5, 6,$ and 7 T, respectively, for $H \parallel c$.

in the latter technique for obtaining maximum accuracy. We also want to emphasize again that *no additional data-filtering techniques* were used to reduce the scattering in the heat-capacity data presented here.

The data shown in Fig. 6 are, within the above-discussed systematic error in the absolute heat capacity ($< 5\%$ at $T = T_c$), in full agreement with published literature values for the specific-heat discontinuity of $\text{YBa}_2\text{Cu}_3\text{O}_7$ near T_c .^{4,7} The excellent relative precision of these data allows us to make a detailed quantitative analysis investigating the temperature and field dependence of the electronic specific heat around T_c , which will be published in a separate publication.¹⁸

V. MEASUREMENTS NEAR THE IRREVERSIBILITY BOUNDARY OF $\text{YBa}_2\text{Cu}_3\text{O}_7$

The irreversibility boundary $H_{\text{irr}}(T)$ in the magnetic phase diagram of cuprate superconductors separates a true zero-resistivity state showing magnetic hysteresis from a state with reversible dc magnetization and dissipative electrical transport properties.¹⁹ It is assumed that in clean samples a melting of the regular vortex lattice into a vortex-liquid phase occurs when crossing $H_{\text{irr}}(T)$ from low to high temperatures (or from small to large magnetic fields, respectively),²⁰ while in more disordered

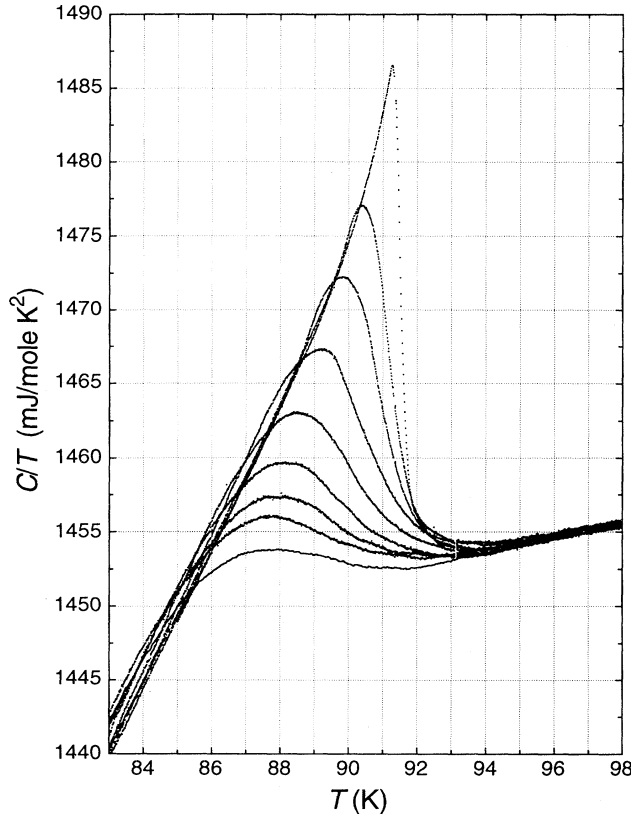


FIG. 6. Specific heat C/T vs T of the $\text{YBa}_2\text{Cu}_3\text{O}_7$ single crystal investigated here, calculated according to Eq. (4) with $k_s/k_r=1$ (see text), for various values of the external magnetic field $H||c$. The magnetic-field values are the same as indicated in the caption of Fig. 5. Note that these specific-heat data are virtually free from an instrumental broadening on the temperature axis.

samples a transition from a vortex-glass phase to a vortex liquid should take place.²¹ Theoretical work supports the idea that the vortex-lattice melting corresponds to a first-order phase transition associated with a jump in entropy S .²² It is not unreasonable to assume that this transition, which is accompanied by an obvious change in translational symmetry, is the only *true* phase transition of the electronic subsystem of copper oxide superconductors occurring at temperatures of the order of T_c and for $H > 0$. The upper critical field $H_{c2}(T)$, known to sharply separate the superconducting from the normal state in other classes of bulk type-II superconductors, may be thought to be replaced in cuprates by a fluctuation-dominated crossover region showing a significant but nevertheless entirely continuous drop in the electronic entropy with decreasing temperature.²³ Measurements of thermodynamic quantities around the irreversibility boundary $H_{\text{irr}}(T)$ of copper oxide superconductors are therefore of utmost interest both from the experimental and from the theoretical point of view.

Recent magnetization $M(T, H)$ experiments for $H||c$ have suggested that the transition to irreversibility in $\text{Bi}_2\text{Sr}_2\text{CaCu}_2\text{O}_8$ below $\mu_0 H \approx 40$ mT is indeed associated

with a jump in M and thus in S ,^{24,25} while corresponding investigations on $\text{YBa}_2\text{Cu}_3\text{O}_7$ did not reveal any magnetization anomaly within the experimental resolution.²⁶ On the other hand, results from resistivity $\rho(H, T)$ measurements on very clean single crystals of $\text{YBa}_2\text{Cu}_3\text{O}_7$, showing a hysteresis in the sharply vanishing $\rho(H, T)$ at $H_{\text{irr}}(T)$, were interpreted as evidence for the occurrence of a first-order transition of the vortex matter also in this compound.²⁷ Other explanations for the origin of such features in the nonequilibrium quantity ρ have been recently suggested, however.²⁸

We aim to demonstrate below that an entropy change ΔS at $H_{\text{irr}}(T)$ should be discernible in heat-capacity data obtained from DTA experiments according to our technique as soon as $\Delta S > 0.05k_B$ per vortex per superconducting layer (where $k_B = 1.38 \times 10^{-15}$ J/K is the Boltzmann constant), for $\mu_0 H = 7$ T parallel to the c axis of the investigated single crystal.

Following our arguments presented in Sec. III, we have to focus on the temperature difference $|T_s - T_r|$ between the sample and the reference specimen which should shift at the hypothetical first-order transition temperature $T^* = T_{\text{irr}}$ by $\Delta T = L/C_s$. If we assume a latent heat $L = \alpha k_B T$ per vortex per superconducting layer associated with a melting transition [with $\alpha \approx 0.3 - 0.4$ (Refs. 22 and 29)], the total latent heat L_v per volume is $L_v = \alpha k_B T B / \Phi_0 s$, where B is the magnetic induction, $\Phi_0 = 2.07 \times 10^{-15}$ V s is the magnetic flux quantum, and s is the distance between the layers. Inserting for this last quantity the distance $s \approx 12$ Å between two double CuO_2 sheets measured along the c axis of $\text{YBa}_2\text{Cu}_3\text{O}_7$, we find that ΔT exceeds our instrumental resolution $\theta \approx 0.2$ mK for $\mu_0 H > 1.6$ T, which is well within the possibilities of our apparatus ($\mu_0 H \leq 7$ T).

To better visualize whether such a shift in $|T_s - T_r|$ is present in our data or not, we fitted the corresponding temperature-dependent $(T_r - T_s)(T)$ data to a fifth-order polynomial covering a temperature window ± 10 K around the magnetically determined irreversibility temperatures $T_{\text{irr}}(H)$ (Ref. 15) (see Fig. 7, inset), and subtracted this smooth function from the original data. In this way, a sudden change in $(T_r - T_s)(T)$ should be clearly visible. In Fig. 7 we present representative data that we obtained for $\mu_0 H = 7$ T, both for cooling the sample in the magnetic field and for a subsequent heating of the specimen above T_{irr} , respectively. For comparison we have also plotted what could be expected if the transition to irreversibility in our sample were of first order. A collection of further data that we measured for magnetic fields down to $\mu_0 H = 3$ T is shown in Fig. 8. From these figures it is obvious that a characteristic indicating a first-order phase transition at T_{irr} is below our detection limit. For $\mu_0 H < 2$ T, the scatter in $T_s - T_r$ exceeds the amplitude of the expected shift in ΔT .

We have demonstrated that our $\text{YBa}_2\text{Cu}_3\text{O}_7$ single crystal does not show a latent heat at the transition to irreversibility within our experimental resolution, which is $0.05k_B T$ per vortex per superconducting layer in $\mu_0 H = 7$ T. This is not really surprising, however, since we know that this particular crystal is twinned within the ab plane.

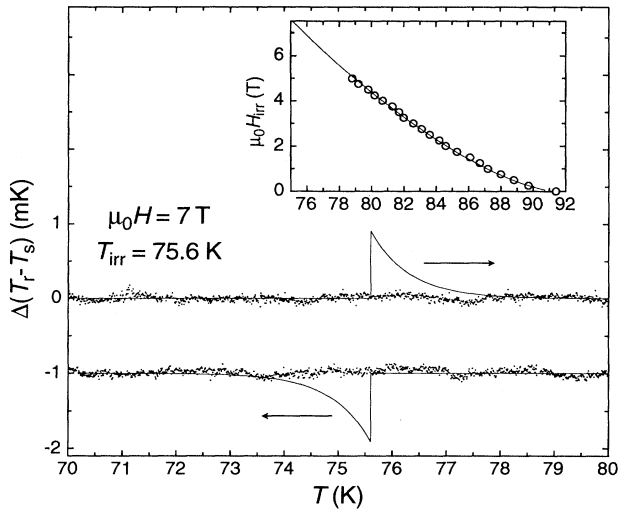


FIG. 7. Variation $\Delta(T_r - T_s)$ vs T of $T_r - T_s$ with respect to a polynomial fit to $(T_r - T_s)(T)$ around the irreversibility temperature T_{irr} , for both cooling and heating the sample in $\mu_0H = 7$ T (see text). For clarity the lower curve has been vertically shifted by -1 mK. The solid line shows a plot of what would be expected if a first-order phase transition occurred at T_{irr} with $L = 0.3k_B T$ per vortex per layer. The magnetically measured irreversibility line obtained on the same sample (Ref. 15) is plotted in an inset, together with a corresponding power-law fit $H_{irr}(T) = H_0(T_c/T - 1)^{1.5}$ used here for estimating T_{irr} for $\mu_0H > 5$ T.

It has been experimentally shown that the sharp resistive drop observed in clean untwinned samples at $H_{irr}(T)$ (Ref. 27) vanishes in the presence of twin boundaries in an $H||c$ geometry.³⁰ We have indeed not observed such sharp resistivity $\rho(T)$ anomalies on the $\text{YBa}_2\text{Cu}_3\text{O}_7$ crystal that we used for the present study.¹⁶ The upper limit for the latent heat L estimated here with a *true thermal experiment* is larger than corresponding limits obtained from torque-magnetometry investigations [$L < 0.003k_B T$ (Ref. 26)]. Rather than having proved the absence of a first-order transition of the vortex ensemble in $\text{YBa}_2\text{Cu}_3\text{O}_7$, we have demonstrated the general applicability of our DTA technique to such delicate thermal investigations.

We finally want to mention the possibility that identifying the parameter s with the distance between multiple CuO_2 sheets for calculating the number of vortex fragments per volume might not be adequate for cuprates, if their effective-mass anisotropy $\gamma = (m_c^*/m_{ab}^*)^{1/2}$ is relatively low. To obtain an idea about the effective length of such vortex segments we want to estimate roughly the number n of layers with thickness s piled up along the c direction that carry such “independent” vortex fragments. For this purpose we compare the Josephson length $\lambda_J = \gamma s$, which indicates the length scale of maximum lateral excursions of a vortex line from one superconducting layer to another, with the intervortex distance $a_0 \approx (\Phi_0/B)^{1/2}$. After a stack of $n = a_0/\lambda_J$ layers, a vortex fragment with length ns may fall out of a

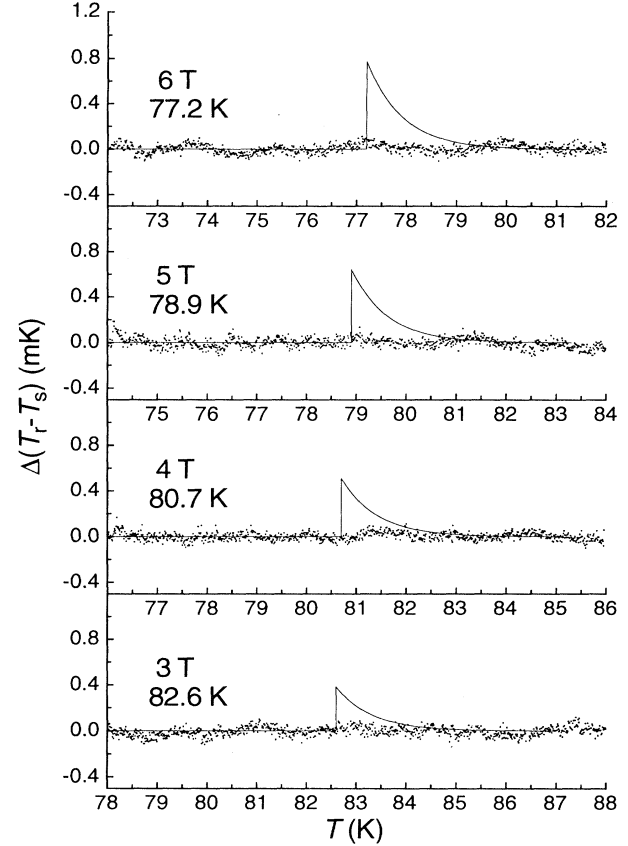


FIG. 8. Variations $\Delta(T_r - T_s)$ vs T obtained when heating the samples in various external magnetic fields after previous field cooling. The meaning of the solid line is explained in the caption of Fig. 7. The numbers indicate the respective values for μ_0H and T_{irr} .

straight line by an entire intervortex distance a_0 . We may use this criterion for defining the length of a vortex segment contributing to the heat of melting [a similar argument fixing $n = 1$ can be used to define the so-called two- to three-dimensional (2D-3D) crossover induction B_{2D} , above which each superconducting layer carries 2D “pancake” vortices]. Inserting realistic parameters for our experiment, i.e., $B = 5$ T, $\gamma = 6$, and $s = 12$ Å, we obtain for $\text{YBa}_2\text{Cu}_3\text{O}_7$ $n \approx 3$. The latent heat L_v per sample volume calculated above might thus be overestimated by this factor. Nevertheless, even a corresponding reduction of L_v accounting for moderate anisotropy does not really invalidate our conclusions since a corresponding smaller shift ΔT in $|T_s - T_r|$ still exceeds the instrumental temperature resolution θ for $\mu_0H > 4.5$ T if $\alpha = 0.3$. In this sense we may still hope to be able to detect a first-order phase transition at $H_{irr}(T)$ in $\text{YBa}_2\text{Cu}_3\text{O}_7$ samples of better quality, if such a transition exists.

VI. CONCLUSIONS

We have described a technique that represents a simple but significant improvement of conventional differential thermal analysis methods. It can be used for measuring

the heat capacity of small samples below room temperature with a very high relative accuracy, $\delta C/C < 0.02\%$. A corresponding experimental setup can alternatively be operated for identifying a first-order phase transition and for measuring an associated latent heat L .

Our experiments on monocrystalline $\text{YBa}_2\text{Cu}_3\text{O}_7$ demonstrate the high quality of the heat-capacity data that can be obtained from such measurements. We have also shown that a latent heat of the order of $L \approx 0.3k_B T$ per vortex per layer at the irreversibility line of $\text{YBa}_2\text{Cu}_3\text{O}_7$ for $H \parallel c$ should be clearly detectable for samples of milligram size. The absence of such a feature in our data, however, may be attributed to sample-quality problems, and can therefore not be considered as a proof for the absence of a first-order transition of the vortex matter at the irreversibility line of $\text{YBa}_2\text{Cu}_3\text{O}_7$ in general.

The technique described here has still some potential for improvements since the accuracy of the measurement is directly related to the precision available for detecting the temperature difference between the sample and the reference specimen. An improvement in thermometry, and/or the use of appropriate data-averaging techniques, may increase the relative accuracy of this DTA technique by an order of magnitude or more.

ACKNOWLEDGMENTS

This work was financially supported by the Schweizerische Nationalfonds zur Förderung der Wissenschaftlichen Forschung. We would like to thank Professor Dr. H. R. Ott for his kind support. We also thank Dr. Th. Wolf for providing the $\text{YBa}_2\text{Cu}_3\text{O}_7$ single crystals.

APPENDIX:

EFFECT OF A NONVANISHING HEAT LINK k_{rs}

In a real experiment, leads to the sample and to the reference object, forming the heat links or electrical connections, have to be perfectly thermally anchored to the heat reservoir. If the temperature difference $T_s - T_r$ is measured with a pair of thermocouples, the wire material connecting the two specimens has also to be chosen to minimize heat transfer between the sample and the reference material. If two wires forming the thermal link unintentionally touch before reaching their connection to the thermal bath, or if the thermocouple wire transfers too much heat, the condition $k_{rs} \ll k_s$ (and k_r , respectively) is no longer fulfilled. Instead of Eqs. (1) we have to consider

$$C_s \dot{T}_s = k_s(T_b - T_s) - k_{rs}(T_s - T_r), \quad (\text{A1a})$$

$$C_r \dot{T}_r = k_r(T_b - T_r) + k_{rs}(T_s - T_r). \quad (\text{A1b})$$

If again $\Delta C = C_s - C_r$, we obtain for the quantity ΔC_0 , calculated from experimental data according to Eq. (2),

$$\Delta C_0 = \frac{k_r}{k_s} \frac{\dot{T}_s}{\dot{T}_r} \left[\frac{\Delta C + C_r(1 - k_s \dot{T}_r / k_r \dot{T}_s)}{1 + k_{rs}/k_s(2 + \dot{T}_s \Delta C / \dot{T}_r C_r)} \right]. \quad (\text{A2})$$

It is obvious that a nonzero k_{rs} leads to a reduction of the apparent heat-capacity difference ΔC_0 by $\approx 2\Delta C k_{rs}/k_s$ if $C_s \approx C_r$ and $k_s \approx k_r$, respectively. It can also be shown that, due to the unwanted heat link k_{rs} , the temperature difference $T_s - T_r$ relaxes as a function of time on the new time scale $\tau_{rs} = C_s / (k_s + 2k_{rs})$. A measurement comparing the time constants τ_{rs} and τ_s can therefore be used as a test for the presence of a large parasitic heat link k_{rs} .

- ¹M. B. Salamon, J. Shi, N. Overend, and M. A. Howson, Phys. Rev. B **47**, 5520 (1993).
- ²B. Zhou, J. Buan, S. W. Pierson, C. C. Huang, O. T. Valls, J. Z. Liu, and R. N. Shelton, Phys. Rev. B **47**, 11 631 (1993).
- ³A. Junod, K. Q. Wang, T. Tsukamoto, G. Triscone, B. Revaz, E. Walker, and J. Muller, Physica C **229**, 209 (1994).
- ⁴E. Janod, A. Junod, K. Q. Wang, G. Triscone, R. Calemczuk, and J. Y. Henry, Physica C **234**, 269 (1994).
- ⁵M. Roulin, A. Junod, K. Q. Wang, E. Janod, and J. Muller, Physica C **244**, 225 (1994).
- ⁶O. Jeandupeux, A. Schilling, and H. R. Ott, Physica C **216**, 17 (1993).
- ⁷N. Overend, M. A. Howson, and I. D. Lawrie, Phys. Rev. Lett. **72**, 3238 (1994).
- ⁸K. A. Moler, D. J. Baar, J. S. Urbach, R. Liang, W. N. Hardy, and A. Kapitulnik, Phys. Rev. Lett. **73**, 2744 (1994).
- ⁹J. W. Loram, K. A. Mirza, J. R. Cooper, and W. Y. Liang, Phys. Rev. Lett. **71**, 1740 (1993).
- ¹⁰S. W. Pierson, J. Buan, B. Zhou, C. C. Huang, and O. T. Valls, Phys. Rev. Lett. **74**, 1887 (1995).
- ¹¹P. F. Sullivan and G. Seidel, Phys. Rev. **173**, 679 (1968).
- ¹²A. Junod, J. Phys. E **12**, 945 (1979).
- ¹³R. Bachman, F. J. DiSalvo, T. H. Geballe, R. L. Greene, R. E. Howard, C. N. King, H. C. Kirsch, K. N. Lee, R. E. Schwall, H. U. Thomas, and R. B. Zubeck, Rev. Sci. Instrum. **43**, 205 (1972).
- ¹⁴For a review, see, e.g., *Differential Thermal Analysis*, edited by R. C. Mackenzie (Academic, London, 1972).
- ¹⁵A. Schilling, H. R. Ott, and Th. Wolf, Phys. Rev. B **46**, 14 253 (1992).
- ¹⁶S. Samarappuli, A. Schilling, M. A. Chernikov, and H. R. Ott, Physica C **201**, 159 (1992).
- ¹⁷G. K. White and S. J. Collocott, J. Phys. Chem. Ref. Data **13**, 1251 (1984).
- ¹⁸O. Jeandupeux, A. Schilling, and H. R. Ott (unpublished).
- ¹⁹K. A. Müller, M. Takashige, and J. G. Bednorz, Phys. Rev. Lett. **58**, 1143 (1987).
- ²⁰A. Houghton, R. A. Pelcovits, and A. Sudbø, Phys. Rev. B **40**, 6763 (1989).
- ²¹M. P. A. Fisher, Phys. Rev. Lett. **62**, 1415 (1989).
- ²²R. E. Hetzel, A. Sudbø, and D. A. Huse, Phys. Rev. Lett. **69**, 518 (1992).
- ²³D. S. Fisher, M. P. A. Fisher, and D. A. Huse; Phys. Rev. B **43**, 130 (1991).
- ²⁴H. Pastoriza, M. F. Goffman, A. Arribère, and F. de la Cruz, Phys. Rev. Lett. **72**, 2951 (1994).
- ²⁵E. Zeldov, D. Majer, M. Konczykowski, V. B. Geshkenbein, V. M. Vinokur, and H. Shtrikman, Nature **375**, 373 (1995).
- ²⁶D. E. Farrell, W. K. Kwok, U. Welp, J. Fendrich, and G. W. Crabtree, Phys. Rev. B **51**, 9148 (1995).

²⁷H. Safar, P. L. Gammel, D. A. Huse, D. J. Bishop, J. P. Rice, and D. M. Ginsberg, *Phys. Rev. Lett.* **69**, 824 (1992).

²⁸W. Jiang, N. C. Yeh, D. S. Reed, U. Kriplani, and F. Holtzberg, *Phys. Rev. Lett.* **74**, 1438 (1995).

²⁹J. Hu and A. H. MacDonald, *Phys. Rev. Lett.* **71**, 432 (1993).

³⁰W. K. Kwok, S. Fleshler, U. Welp, V. M. Vinokur, J. Downey, G. W. Crabtree, and M. M. Miller, *Phys. Rev. Lett.* **69**, 3370 (1992).

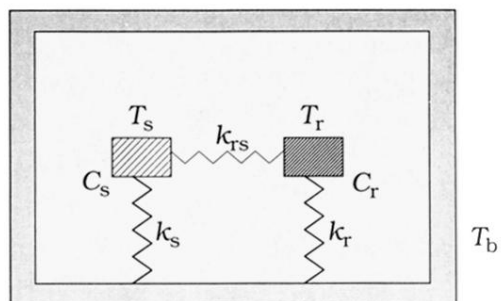


FIG. 1. Schematic view of the standard DTA configuration used for the present work. The sample (heat capacity C_s , temperature T_s) and a reference sample (heat capacity C_r , temperature T_r) are thermally connected to a heat reservoir (temperature T_b) via the heat links k_s and k_r . The effect of an additional unwanted link k_{rs} is discussed in an Appendix to this paper.